Structure of Concentrated-Flux-Type Interior Permanent-Magnet Synchronous Motors Using Ferrite Permanent Magnets

Hae-Joong Kim, Doo-Young Kim, and Jung-Pyo Hong

Department of Automotive Engineering, Hanyang University, Seoul 133-791, Korea

Interior permanent magnet synchronous motors (IPMs) usually use NdFeB for achieving high-torque and high-efficiency performance. This paper reviews the performance of concentrated-flux-type ferrite magnet motors (CFFMs) that use ferrite, as an alternative to the general type of IPMs that use NdFeB. A structure to reduce the motor volume and improve the torque density of CFFMs is suggested in this paper. The characteristics of CFFMs for different rotor types are analyzed. The motor parameters are analyzed. Using 2-D finite element analysis (FEA), the efficiency and size of the CFFMs are compared with each other. This paper discusses the results of stress analysis for each rotor type using 2-D FEA. Finally, it suggests a CFFM structure to replace the general type of IPMs that use NdFeB. The proposed *LC*-type has the highest torque density among all the ferrite rotor types. It is seen that the proposed *LC*-type ferrite-model replacement for the Nd model is the best choice of all the types.

***Index Terms*— AC motors, concentrated-flux type, ferrite, permanent magnet, stress analysis.**

I. Introduction

VARIOUS efforts have been made to mitigate global warming and energy problems. In particular, interior permanent magnet synchronous motors (IPMs) that use rare-earth permanent magnets have attracted considerable attention [1]. However, recently, the prices of rare-earth elements have increased and they are also subject to export restrictions. To reduce dependence on such elements, various motors without rare-earth materials, such as induction motors, switching flux PM motors, synRMs, and concentrated-flux-type ferrite magnet motors (CFFMs) are being developed [2]–[5]. Ferrite magnets are now being considered as a substitute for rare-earth elements because of the aforementioned situation. Although the residual flux density of ferrite magnets is one-third of a rare-earth magnet, the cost is only about one-tenth. In addition, a stable supply is available [6]–[11]. However, to apply ferrite magnets in a way such that a satisfactory performance is obtained, the magnetic structure should be newly designed to enhance energy density because of the relatively low-residual flux density of the ferrite PM [12]. To solve this problem, improvements in the stator and rotor structure of the motor are needed. This paper suggests a structure to reduce the motor volume of the CFFM and improve the torque density. The back electromotive force (back-EMF) and saliency ratio are calculated and compared using 2-D, and 3-D finite element analysis (FEA) on CFFMs with different structures. In addition, stiffness analysis is conducted to confirm the mechanical characteristics. The motor characteristics and torque densities are confirmed using a d- and q-axes equivalent circuit.

II. Comparison of the Structure and Characteristics of the Motor

Fig. 1 shows the design plan for improving CFFMs. There are ways to increase the flux per pole and ways to increase saliency ratio in the design plan for the torque density improvement and cost reduction. To increase the flux per pole, an increase in the thickness and/or area of the permanent magnet or an increase the cross section of the air gap is needed. To increase the saliency ratio, an increase in the number of permanent-magnet layers or an increase in the thickness of the permanent magnet is needed. In Fig. 2, the Nd model is the drive motor for a 1.5 kW compressor. The Nd model uses NdFeB and the other models used ferrite as the permanent-magnet material.

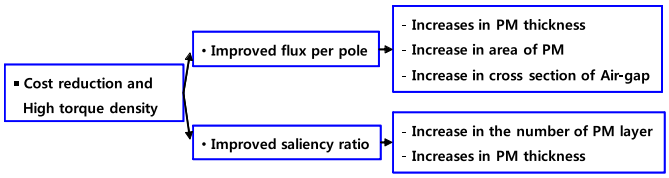

Fig. 1. Plan for torque density improvement and cost reduction of CFFMs.

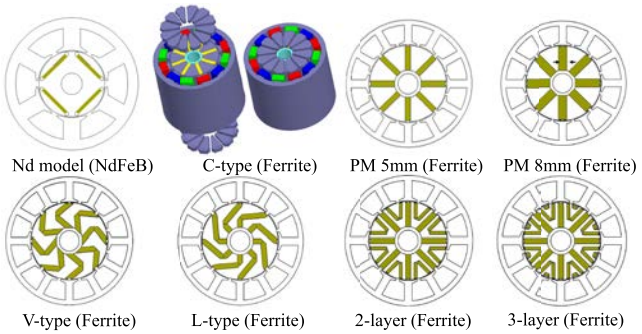

Fig. 2. Concentrated-flux-type ferrite magnet motor.

The C-type of the CFFM uses an air gap at the top face, bottom face, and the side of the rotor to increase the cross section of the air gap. The cap is a part of the stator and is in contact with the tooth of the stator. This increases the flux per pole. Fig. 3 shows the side view of a C-type. The cap material is a soft magnetic composite (SMC). The SMC materials are magnetically isotropic and hence ideal for constructions of electrical machines with complex structure and 3-D magnetic flux path. This removes the well-known restrains on the conventional laminated machines, e.g., the magnetic flux must flow within the lamination plane to avoid excessive eddy current loss [13]. The cap is fixed to the housing and helps in

Manuscript received March 7, 2014; revised May 5, 2014; accepted May 8, 2014. Date of current version November 18, 2014. Corresponding author: H.-J. Kim (e-mail: kimheajoong@hanmail.net).

Color versions of one or more of the figures in this paper are available online at http://ieeexplore.ieee.org.

Digital Object Identifier 10.1109/TMAG.2014.2323818

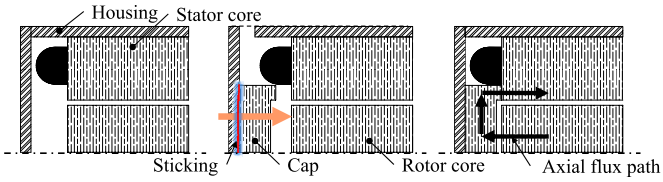

Fig. 3. Concentrated-flux-type ferrite magnet motor C-type.

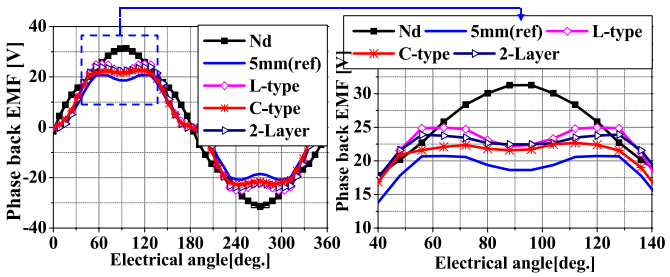

Fig. 4. Phase back-EMF waveform (2-D FEA).

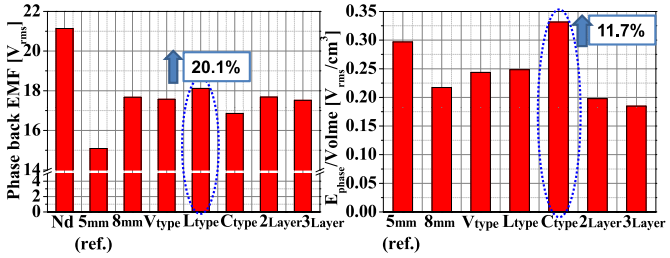

Fig. 5. Phase back-EMF and EMF/PM volume.

forming the axial flux path. The model labeled PM-5 mm is the general CFFM structure where the thickness of the permanent magnet is 5 mm. The thickness of the permanent magnet in the model labeled PM-8 mm is 8 mm, which is the maximum permanent magnet thickness for the combination part of the rotor core. If the permanent magnet thickness is increased, both the flux per pole and saliency ratio increases.

The V-type and L-type are the models that increase the cross section of the permanent magnet; the L-type has a greater flux saturation of the rotor than the V-type. 2-layer and 3-layer models increase the number of the permanent magnet layers. The saliency ratio in these structures is higher than that in the other models. The outer diameters of the stator and rotor, series-turns per phase, and conductor diameter of the coil of all models are the same.

Fig. 4 shows the phase back-EMF waveform through the 2-D FEA of each motor when the stack lengths of the motors are identical. Fig. 5 shows the analysis result of the phase back-EMF and phase back-EMF per PM volume. The phase back-EMF in the Nd-model is higher than that in all other models because the residual magnetic flux density (1.3 T) of the permanent magnet is high. The permanent magnet residual magnetic-flux density of the ferrite models is 0.38 T. The increase in the phase back-EMF of the L-type is the highest with an increase of 20.1% over the PM-5 mm model. In addition, the L-type has a higher phase back-EMF per PM volume than the PM-8 mm model, which has a greater permanent magnet thickness. We see that the L-type provides better motor-torque-density improvement and cost reduction than the PM-8 mm model. In terms of the phase back-EMF per

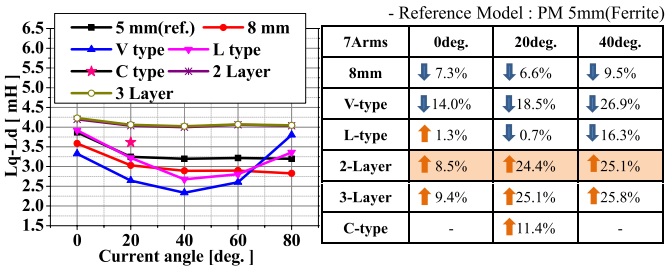

- Reference Model : PM 5mm(Ferrite)

7Arms	0deg.	20deg.	40deg.
8mm	⬇ 7.3%	⬇ 6.6%	⬇ 9.5%
V-type	⬇14.0%	⬇18.5%	⬇26.9%
L-type	⬆ 1.3%	⬇ 0.7%	⬇16.3%
2-Layer	⬆ 8.5%	⬆24.4%	⬆25.1%
3-Layer	⬆ 9.4%	⬆25.1%	⬆25.8%
C-type	-	⬆11.4%	-

Fig. 6. Values of difference between d-axis inductance and q-axis inductance (2-D FEA).

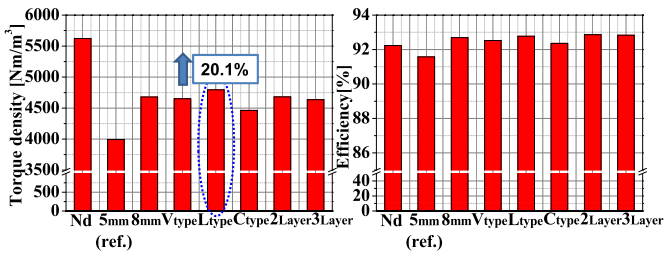

Fig. 7. Torque density and efficiency.

PM volume, the C-type displays the highest increase (increase of 11.7%). Since the C-type increases the cross section of the air gap, it does not increase the PM volume, but increase the phase back-EMF, therefore, it is useful for achieving cost reduction. The 2-layer and 3-layer models have a lower phase back-EMF per PM volume than the other models. Although the PM volume of the 3-layer model is higher than that of the 2-layer model, the phase back-EMF decrease owing to flux saturation of the rotor.

The difference ($Ld - Lq$) between d-axis inductance, Ld, and q-axis inductance, Lq, has a direct effect on the reluctance torque. Fig. 6 shows the $Ld - Lq$ for each model. The 2-layer and 3-layer models have the highest $Ld - Lq$ values. This means that the reluctance torque is high and it is thought to be beneficial for designing high-torque, high-current motors, such as traction motors. PM-8 mm model, where the $Ld - Lq$ value was expected to increase, showed contrasting results; the q-axis inductance decreased because of the narrow q-axis flux path. However, the PM-8 mm model is expected to improve the $Ld - Lq$ value by little improvement in the structure. In the L-type and V-type, the $Lq - Ld$ is higher than that of the PM-5 mm standard model owing to the increase of in the d-axis inductance. Since Ferrite models have a smaller phase back-EMF than the Nd-models, the stack length should increase to deliver the same output. Fig. 7 shows the torque density and efficiency for each model with the same phase back-EMF, under the same output condition. The L-type that showed the highest phase back-EMF also had the highest torque density. All models are nearly 92.5% efficient, except for the PM-5 mm standard model.

III. Rotor Stress Analysis of Motor Structures

The rotor shape of the CFFM is structurally weaker than the rotor shape of general IPMs for high-speed driving. Therefore, considering the stress when designing the rotor shape for the CFFM is very important. The CFFM causes significant leakage-flux inside the rotor. The width of the bridge connecting the rotor core should be reduced to reduce the leakage-

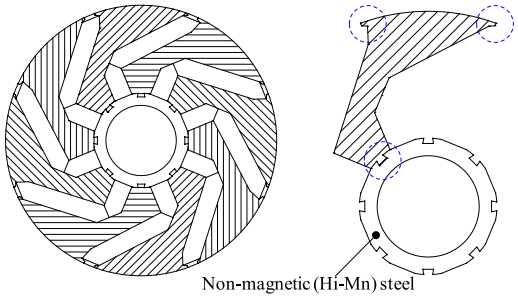

Fig. 8. Rotor core and non-magnetic material shape of the *L*-type CFFM.

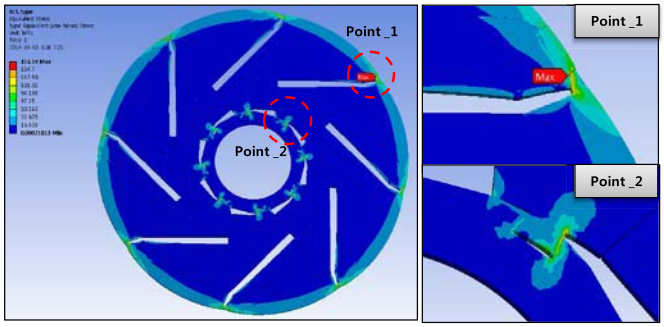

Fig. 9. Rotor stress analysis for the CFFM *L*-type.

flux inside the rotor, but that makes it structurally weak during high-speed driving. Therefore, the design presented in this paper used a non-magnetic material for improving the structural stability of the rotor and for the reduction of the leakage flux. The non-magnetic material used was Hi-Mn steel. Hi-Mn steel has a very high yield strength and tensile strength in comparison with other materials. There is a groove to fix the rotor core in the non-magnetic material. Non-magnetic material steel is fixed to the shaft and each rotor core is fixed to the non-magnetic steel, and the ferrite is inserted between each rotor core.

Fig. 8 shows the rotor core of the CFFM and the shape of the non-magnetic material. Since the groove of the non-magnetic material is shaped as a trapezoid, the rotor core has to be inserted axially and the inserted rotor core is not separated radially. The part marked with a circle in Fig. 8 is where the stress is highest during high-speed driving. Fig. 9 shows the stress analysis result for the *L*-type through 2-D FEA at a driving speed of 10 000 r/min. The core material S18 was used as the material of the rotor core. The yield strength of S18 is 275 MPa. The red circle in Fig. 9 is where the stress was shown to be highest. When the driving speed is 10 000 r/min, the maximum stress in the rotor core of the *L*-type is 151 MPa, and the safety factor is 1.82. Fig. 10 shows the 2-D FEA stress values for each rotor shape. The maximum stress in the PM-5 mm model, the standard model, is 137 MPa. The *L*-type results show asymmetric stress at point 1 and point 2 owing to the asymmetry in the rotor core and magnet shape. Therefore, the *L*-type is subject to a slightly higher stress than the other types.

IV. CFFM Prototype and Experimental Results

Since the *L*-type has the highest phase back-EMF of all the rotor types, the torque density is also the highest. Therefore, it is the most suitable ferrite model to replace the Nd model.

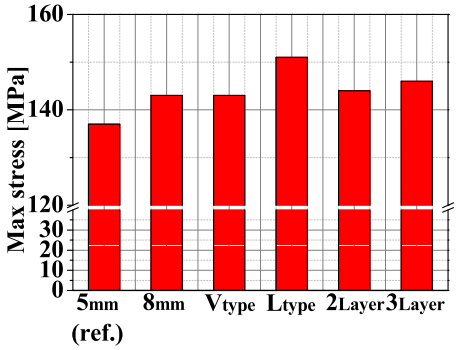

Fig. 10. Max stress of rotor.

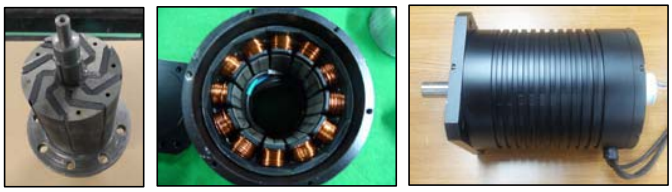

Fig. 11. CFFM prototype. (a) Rotor. (b) Stator. (c) Final assembly.

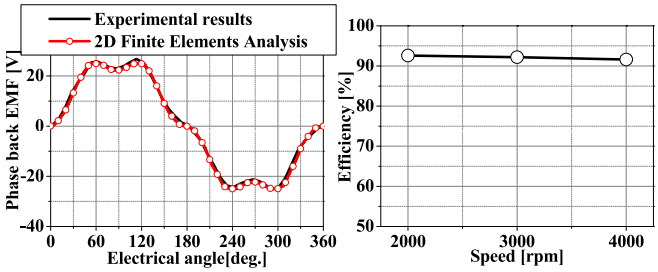

Fig. 12. Phase back EMF and efficiency for the prototype.

We made a prototype and performed no-load and load testing to validate the performance of the *L*-type. Fig. 11 shows the rotor, stator, and final assembly of the *L*-prototype.

Fig. 12 shows the no-load test and load test results for the *L*-prototype at a driving speed 1000 r/min. The test result for no-load back-EMF and the 2-D FEA analysis results had a difference of ∼2%. The load test efficiency was measured to be ∼92% in the 2000–4000 r/min speed range. The size of the ferrite PM-5 mm model is ∼141% the Nd-model size. On the other hand, the size of the ferrite *L*-type is ∼117% the Nd-model size. That is, the *L*-type is most suited to replace the Nd-model as the Ferrite model.

V. CFFM Structure Proposal

As described earlier, the *L*-type improves the motor torque density and the *C*-type reduces the permanent magnet use. This paper suggests an *LC*-type CFFM rotor structure that combines the merits of the two types. Fig. 13 shows the shape of the *LC*-type. The rotor shape is identical to that of the *L*-type and a cap is attached to the housing like in the *C*-type. The shape of the cap applied to the *L*-type should be similar to the rotor core in order to best secure the axial flux. Since the cap is fixed, an alternating magnetic field generated during high-speed driving, resulting in eddy current loss. Since the flux flows axially from the cap to the rotor, using a laminating

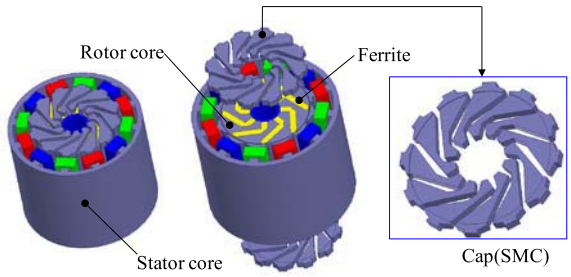

Fig. 13. *LC*-type concentrated-flux-type ferrite magnet motor.

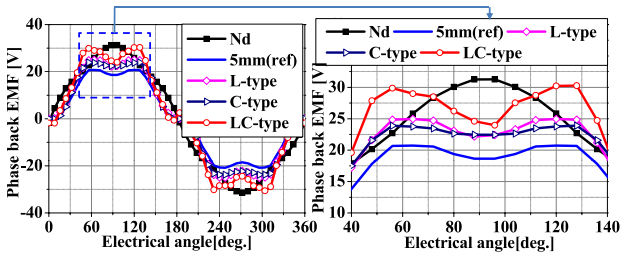

Fig. 14. Phase back EMF waveform for the CFFM (2-D FEA).

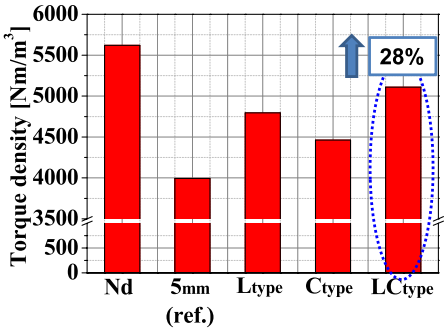

Fig. 15. Torque density.

core, causes a large eddy current loss. Therefore, we think that the SMC will be appropriate as the cap material. Fig. 14 shows the results for the phase back-EMF in the *LC*-type and other rotor types. The phase back-EMF of the *LC*-type was calculated using 3-D FEA and 2-D FEA was used for the other models. The FEA analysis condition is 1000 r/min at 80°. The phase back-EMF of the *LC*-type is higher than that of the *L*-type by ∼7.2%. The phase back-EMF per PM volume is higher by ∼12.5%. The phase back-EMF of the *LC*-type is smaller than that of the Nd model by ∼8.6%. Fig. 15 shows the torque density results for every model at the same output level. The torque density of the *LC*-type is higher than that of the standard PM-5 mm model by ∼28%. The size of the ferrite *LC*-type is ∼110% of the Nd model size. That is, using the ferrite *LC*-type to replace Nd, a PM material of higher residual flux density, we can make deliver the same output with only a 10% penalty in size.

VI. Conclusion

This paper proposed a structure to reduce the motor volume of CFFMs and to improve the torque density. According to the review, the phase back-EMF is the most beneficial for torque density improvement. The *L*-type shows the highest Phase back-EMF among all the types. The phase back-EMF per PM volume are most beneficial for cost reduction, and the *C*-type displays the highest phase back-EMF per PM volume. The 2-layer model is thought to be beneficial for designing a high-torque, high-current motor because the $Ld - Lq$ is large. The proposed *LC*-type has the highest torque density among the ferrite rotor types. The results indicate that the *LC*-type is the best ferrite model to replace the Nd model.

Acknowledgment

This work was supported by the Energy Efficiency and Resources of the Korea Institute of Energy Technology Evaluation and Planning through the Ministry of Knowledge Economy, Korea Government, under Grant 2012T100201723.

References

[1] K. Sone, M. Takemoto, S. Ogasawara, K. Takezaki, and H. Akiyama, "A ferrite PM in-wheel motor without rare earth materials for electric city commuters," *IEEE Trans. Magn.*, vol. 48, no. 11, pp. 2961–2964, Nov. 2012.

[2] W. Kakihara, M. Takemoto, and S. Ogasawara, "Rotor structure in 50 kW spoke-type interior permanent magnet synchronous motor with ferrite permanent magnets for automotive applications," in *Proc. IEEE ECCE*, Sep. 2013, pp. 606–613.

[3] S.-I. Kim, J. Cho, S. Park, T. Park, and S. Lim, "Characteristics comparison of a conventional and modified spoke-type ferrite magnet motor for traction drives of low-speed electric vehicles," *IEEE Trans. Ind. Appl.*, vol. 49, no. 6, pp. 3048–3054, Nov./Dec. 2013.

[4] A. Fasolo, L. Alberti, and N. Bianchi, "Performance comparison between switching-flux and IPM machine with rare earth and ferrite PMs," in *Proc. 20th IEEE ICEM*, Marseille, France, Sep. 2012, pp. 731–737.

[5] S. Ooi, S. Mormoto, M. Sanada, and Y. Inoue, "Performance evaluation of a high power density PMASynRM with ferrite magnets," *IEEE Trans. Ind. Appl.*, vol. 49, no. 3, pp. 1308–1315, May/Jun. 2013.

[6] S. Ishii, Y. Hasegawa, K. Nakamura, and O. Ichinokura, "Characteristics of novel flux barrier type outer rotor IPM motor with rare-earth and ferrite magnets," in *Proc. ICRERA*, Nov. 2012, pp. 1–4.

[7] T. Sun, S.-O. Kwon, J.-J. Lee, and J.-P. Hong, "Investigation and comparison of system efficiency on the PMSM considering Nd-Fe-B magnet and ferrite magnet," in *Proc. 31st Int. Telecommun. Energy Conf.*, pp. 1–6, Oct. 2009.

[8] I. Petrov and J. Pyrhonen, "Performance of low-cost permanent magnet material in PM synchronous machines," *IEEE Trans. Ind. Electron.*, vol. 60, no. 6, pp. 2131–2138, Jun. 2013.

[9] L. Fang, J.-W. Jung, J.-P. Hong, and J.-H. Lee, "Study on high-efficiency performance in interior permanent-magnet synchronous motor with double-layer PM design," *IEEE Trans. Magn.*, vol. 44, no. 11, pp. 4393–4396, Nov. 2008.

[10] E. Armando, P. Guglielmi, M. Pastorelli, G. Pellegrino, and A. Vagati, "Accurate magnetic modelling and performance analysis of IPMPMASR motors," in *Proc. IEEE-IAS Annu. Meeting*, Sep. 2007, pp. 133–140.

[11] P. Zhang, G. Y. Sizov, D. M. Ionel, and N. A. O. Demerdash, "Design optimization of spoke-type ferrite magnet machines by combined design of experiments and differential evolution algorithms," in *Proc. IEEE IEMDC*, Chicago, IL, USA, May 2013, pp. 958–964.

[12] S.-M. Jang, H.-J. Seo, Y.-S. Park, H.-I. Park, and J.-Y. Choi, "Design and electromagnetic field characteristic analysis of 1.5 kW small scale wind power generator for substitution of Nd-Fe-B to ferrite permanent magent," *IEEE Trans. Magn.*, vol. 48, no. 11, pp. 2933–2936, Nov. 2012.

[13] Y. Guo, J. Zhu, H. Lu, Z. Lin, and Y. Li, "Core loss calculation for soft magnetic composite electrical machines," *IEEE Trans. Magn.*, vol. 48, no. 11, pp. 3112–3115, Nov. 2012.